ACTA MECHANICA SINICA, Vol.8, No.3, August 1992 ISSN 0567-7718
Science Press, Beijing, China
Allerton Press, INC., New York, U.S.A.

AERODYNAMIC HEATING IN THE REGION OF SHOCK AND TURBULENT BOUNDARY LAYER INTERACTION INDUCED BY A CYLINDER

Tang Guiming (唐贵明) Yu Hongru (俞鸿儒)
(*Institute of Mechanics, Chinese Academy of Sciences, Beijing* 100080, *China*)

ABSTRACT: Detailed distributions of heat flux in the region of shock wave and turbulent boundary layer interaction induced by a cylinder were measured in the shock tunnel. Oil flow patterns and Schlieren photographs were taken. Empirical relations were given for determining separation shock angle, peaks of heat flux and their locations on both cylinder leading edge and flat plate surface, and other characteristic parameters of the interaction region.

KEY WORDS: shock wave, boundary layer, aerodynamic heating

I. INTRODUCTION

In high speed vehicle design, the shock-turbulent boundary layer interaction heating augmentation induced by protuberance is one of the most severe problems. For three-dimensional protuberance the invisid-viscous interaction flow makes the analytical prediction very difficult, even though the flowfields have been described by several authors.[1-5] Experimental data on protuberance interaction heat flux are very limited particularly for hypersonic turbulent flow. Lack of heat flux measurements and its practical importance promoted this study. Besides measurements of heat flux, a new oil flow technique for short duration facilities was developed to observe the direction of the flow on the model surface. The data obtained from these tests and other investigations were used to form the relations for calculating the peaks of heat flux and their locations on both the leading edge of cylinder and the surface of flat plate, and other characteristic parameters in the interaction regions.

II. EXPERIMENTAL TECHNIQUE

The 1.2m Shock Tunnel The tests were conducted in the 1.2m shock tunnel at Institute of Mechanics, Chinese Academy of Sciences. The tunnel consists of a shock tube, a nozzle, a test section and a vacuum tank as shown in Fig.1. In these tests, the free stream Mach number ranged from 5 to 9, the corresponding Reynolds number ranging from 2 to 6×10^7/m with the test time of about 5 to 7ms.

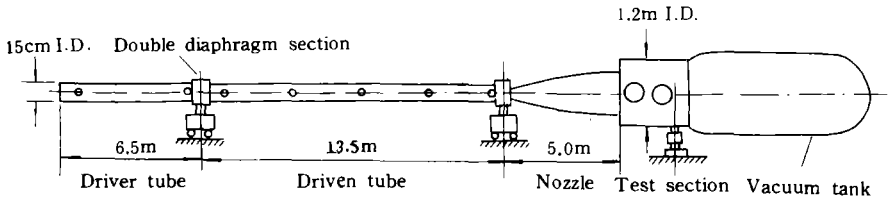

Fig.1 Schematic of the 1.2m shock tunnel

Model A flat plate, 30cm wide by 70cm long, was mounted near the test section axial line. The boundary layer on the model surface starts upstream far from separation initiation to transform to turbulence. The cylinder was mounted on the plate surface at 50cm from the

Received 7 March 1991

plate leading edge. The height of the cylinder may be adjusted from 12 to 20cm and the cylinder may be inclined with an angle from 0 ° to 30 °. The disc of 15cm diameter was inlaid with a series of thin film thermometer arranged in a column. which was a part of the flat plate, and could rotated around the cylinder center. Thus the heat flux distributions at any azimuth can be measured conveniently.

Heat Transfer Instrumentation Thin film resistance thermometer in the form of a strip approximately 0.2mm wide by 2mm long was used as the heat flux measuring element. During the tests a constant current of 20 milliampere passed through the gage. The value of the heat flux was obtained from the film response processed by RC analogue network[6]. The test data were recorded with an A/D converter and processed with the microcomputer.

Flow Visualization on Model Oil flow patterns and Schlieren photographs were taken for typical models. The oil flow technique has been extensively applied to the test in the long duration facilities[2,3]. A new oil flow technique for transient flow was developed to observe the flowfield on the model surface. The oil mixture was made of titanium dioxide dust and silicon oil. The models were painted black and small mixture dots were spread on the surface of the flat plate to visualize the direction of shear force.

III. RESULTS AND DISCUSSION

1. Heat flux distribution and flow pattern on the symmetric plane

The heat flux distributions on the symmetric plane of interaction region for $M_1=5.2$ are shown in Fig.2a. The heat flux data on the leading edge of the cylinder and on the surface of the flat plate are normalized by the undisturbed value on the cylinder leading edge q_s and the local plate value q_1 respectively. The oil flow pattern (Fig.3) show that the interaction of the bow shock induced by the cylinder with the turbulent boundary layer on the plate causes widespread upstream and lateral separations. The impingement of separation shock on the bow shock (Fig.4) results in a lambda shock. The heat flux on the surface of the plate ahead of the cylinder starts to rise at $X_s=1.9d$, reaches a plateau value $q_{p1}=2.8q_1$ at $X_{a1}=0.8d$, goes through a large dip at about $X_{s1}=0.58d$ and then rises sharply to a higher peak $q_{pk}=25q_1$ at $X_a=0.12d$, after which rapidly drops to a low value $q=8.9q_1$ at the foot of the cylinder. The heat flux distribution along the cylinder leading edge from the foot to $Z_p=0.22d$ decreases from $q=q_s$ to $0.4q_s$, after which rises to a short plateau at $Z_r=0.5d$, and then increases steeply

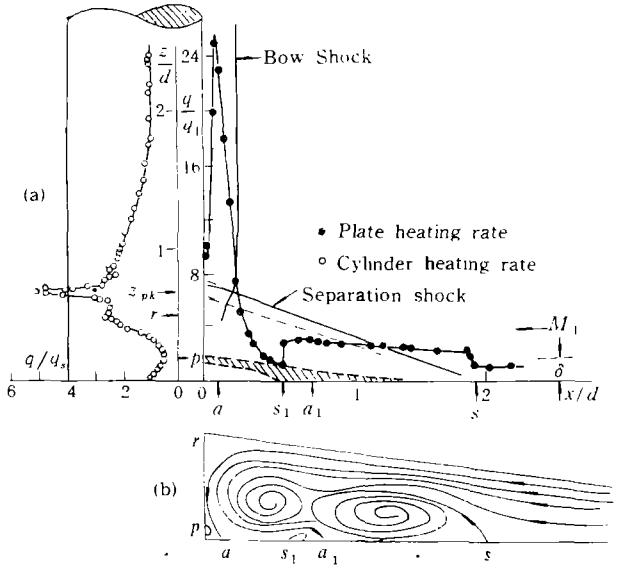

Fig.2 heat flux distributions (a) and imaginary scheme (b) of vortices on the symmetric plane

to attain a higher peak $q_{pk}=5q_s$ at $Z_{pk}=0.67d$. After the peak point, it drops and returns to the undisturbed value q_s.

The maximum heat flux on the cylinder is considered to be due to the existence of the interaction between the bow shock and the separation shock. The height of the peak position is nearly equal to the height of triple point of the lambda and the impingement point of the jet.

The multiple peak shape of the heat flux distribution in the symmetric plane of the separation region is related to the multiple vortex structure. Sedney[3] imagined that there are four vortices in the separation region. The comparison of Fig.2a with Fig.2b shows that three pair of separation and attachment points (s, r; p, a; s_1, a_1) in the flow field correspond to the three pair of valley and peak positions of heat flux distributions (x_s, z_r; z_p, x_a; x_{s1}, x_{a1}) respectively. It is obvious that the heat flux rises to a high value where the stream line impinges the wall and it drops to a low level where the stream line leaves the wall.

The plateau heat flux q_p/q_1 on the flat plate for turbulent interaction is insensitive to Mach number and Reynolds number. The plateau heat flux q_p is equal to $(2.8\pm0.4)q_1$ in the range of $M_1=5$ to 9 and $Re=(1-3)\times10^7$ m.

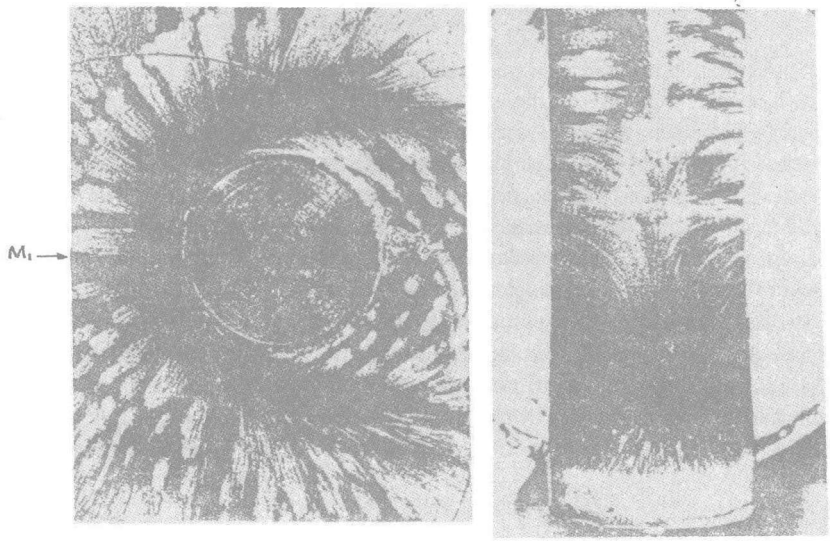

(a) Plate surface (b) Windward surface of cylinder

Fig.3 Oil flow patterns, $M_1=7.8$, $Re=3.5\times10^7$/m, $h/d=3$

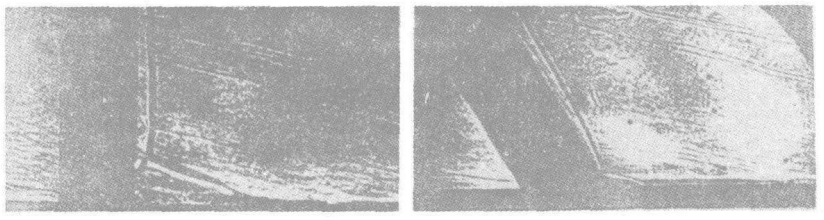

Fig.4 Schlieren pictures, $M_1=5.2$, $Re=2.3\times10^7$/m, $h/d=3$

2. Heat flux peaks on the flat plate

The test results show that the maximum-peak of the heat flux on the flat plate is very sensitive to Mach number. For example, the maximum-peak at the symmetric line is 46 times over the undisturbed plate value at $M_1=9$, 31 times over that at $M_1=6.6$ and 25 times over that at $M_1=5.2$. The variation of the maximum-peak with Mach number and Reynolds

number can be expressed by the approximate expression[7].

$$q_{pk}/q_1 = 1 + 25M_1^{1.8}Re^{-0.2} \tag{1}$$

where the empirical constant are determined on the basis of the present data. The comparison of the calculated values with the measured data is given in Fig. 5. The data obtained from Burbank are lower than the value calculated according to formula (1).

The heat flux distributions along various azimuth lines, which are similar to those along the plate central line, are shown in Fig.6. The locus of the peak positions obtained from the heat flux distributions around the cylinder is shown in Fig.7a. The locus is a semicircle with a radius of $0.74d$ and its center locates $0.13d$ downstream from the cylinder center. The locus is very close to the attachment line observed from the oil flow pattern (Fig. 3a). The peaks on the plate decrease laterally downstream from the central line. The variation of the peak value along the locus is expressed as follows

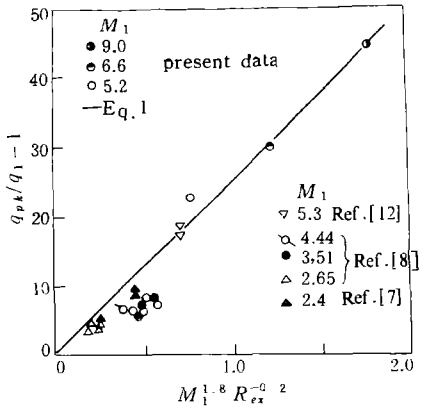

Fig.5 Comparison of calculated value with measured data of heat flux peaks on flat plate

$$(q_{pk}/q_1)_\psi / (q_{pk}/q_1)_{\psi=0} = \cos(\psi - \arcsin(0.18\sin\psi)) \tag{2}$$

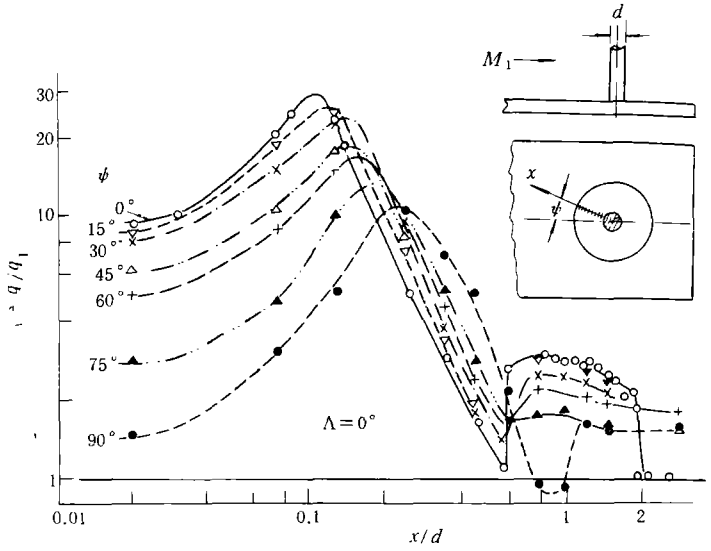

Fig.6 Heat flux distributions on plate along different azimuth angles ($M_1 = 5.2$, $h/d = 3$)

The comparison of the calculated values with the measured data is shown in fig. 7b. It shows a good agreement for $< 80°$. The locus of the valley position on the plate is also shown in Fig. 7a. The data from Ref.[8] are also shown in the figure and are in good agreement with the present results.

3. Characteristic parameters in symmetric plane

The discussed characteristic parameters in the symmetric plane of the interaction region include the separation shock angle θ_s, the deflected angle θ_d of the flow behind the separation shock wave, the separation distance x_s, the position of the maximum peak of the heat flux on the flat plate x_a, the height of the maximum heat flux peak point z_{pk} and the minimum heat flux point z_p on the leading edge of cylinder. The dependence of these characteristic

parameters on Mach number is shown in Fig.8. The following conclusions can be drawn from the figure.

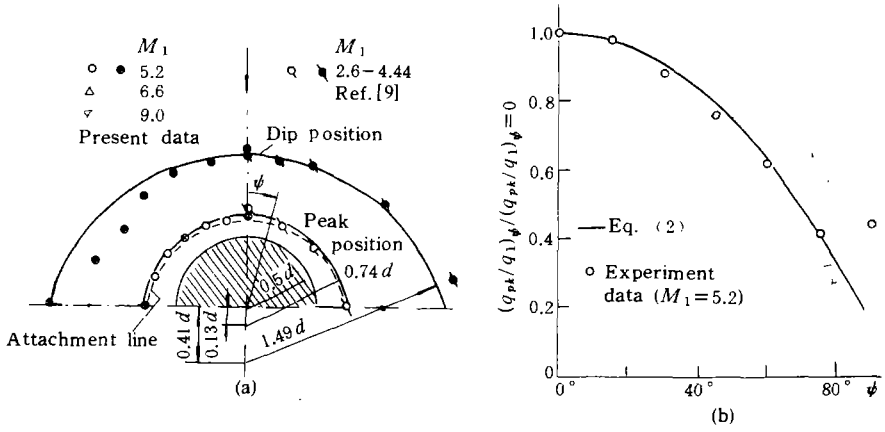

Fig.7 Loci of peak & valley, peak distribution on plate around cylinder

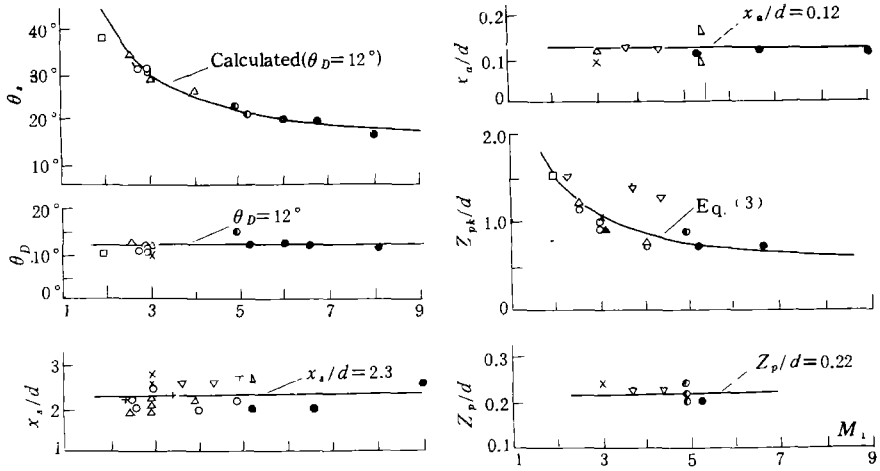

Fig.8 Characteristic parameters on symmetric plane

+ Ref.[3] Δ Ref.[4] ○ Ref.[5] ∇ Ref.[9] × Ref.[11] △ Ref.[12]
◐ Ref.[13] ○ Ref.[14] ⊤ Ref.[15] □ Sykes ● present data

The separation shock angle θ_s and the height of the peak point on the leading edge of the cylinder z_{pk}/d decrease with increasing Mach number of the free stream and approach gently to asymptotic values. The latter can be estimated by the height of the triple point of the lambda shock Z_{tr}/d.

$$z_{pk}/d \approx z_{tr}/d = (x_s/d - B/d)\tan\theta_s \tag{3}$$

where $B/d = 0.193\exp(4.76/M_1^2)$ is the standoff distance of the cylinder bow shock wave[10].

The flow deflected angle θ_d behind the separation shock wave, the turbulent separation distance x_s, the position of the maximum heat flux peak x_a on the plate and the height of the minimum heating point on the cylinder z_p are roughly independent of Mach number and Renolds number of free stream.

4. Effect of cylinder backswept

The strength of the bow shock wave ahead cylinder, the extent of the separation region and therefore the heat flux both on the flat plate and on the cylinder are reduced by the backward sweep of the cylinder. For sweep angle of $\Lambda = 0°$, 15°, 30°, the heights z_{tr} of the triple point of lambda shock wave are 0.66, 0.36, 0.27 and the separation distance s/d are 1.9, 1.2, 0.8

at $M_1=5.2$, respectively.

The effects of backswept on the heat flux both on the leading edge of cylinder and on the central line of the flat plate are shown in Fig.9 and Fig.10. As may be seen from the figures, the heat flux and the height of the peak point on the cylinder leading edge are decreased obviously when the cylinder sweeps back from 0 ° to 30 °. Similarly, the heat flux peak on the plate central line as well as the disturbed region decrease with the increasing backswept of the cylinder. But the plateau heat flux on the plate has a slight variation. The effect of the cylinder backswept on the heat flux peak along the plate central line is shown in Fig.11. It seems that the sweep effect depends weakly on Mach number.

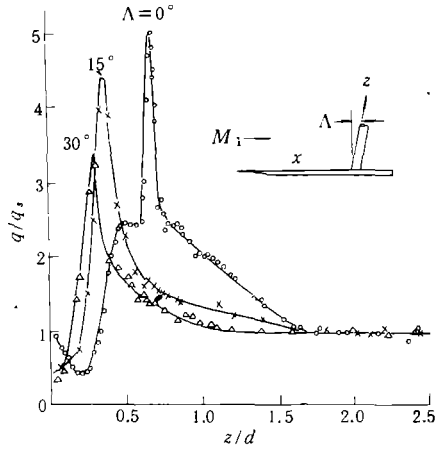

Fig.9 Heat flux distribution along leading edge of swept cylinder

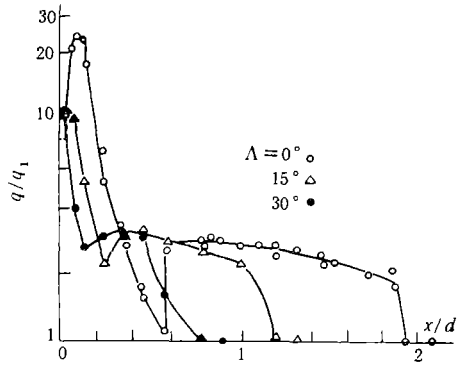

Fig.10 Central line heat flux distribution ahead of a swept cylinder, $M_1=5.2$

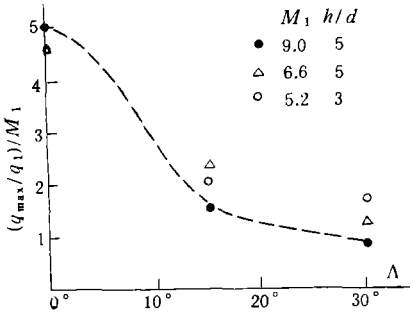

Fig.11 Effect of cylinder sweep on heat flux peak at plate central line

IV. CONCLUSIONS

The aerodynamic heating environment in the region of the shock wave and the turbulent boundary layer interaction induced by a cylindrical protuberance is extremely severe especially for high Mach number. The maximum heat flux along the plate central line ahead of the cylinder can be calculated according to formula (1) and it is 46 times over the undisturbed local value at $M_1=9$. The position of the maximum heating point is not at the foot of the cylinder but instead at a distance of about 0.12 cylinder diameter upstream from it. The peaks of the heat flux decrease laterally downstream from the central line. The locus of the heat flux peaks at different azimuth on the plate is approximately a semicircle.

The multiple peak shape of the heat flux distributions in the interaction region is related to the multiple vortex structure. The separation and attachment points in the disturbed flow

field correspond to the valley and peak heating points, respectively.

The separation shock angle and the height of the peak point on the cylinder's leading edge decrease with increasing Mach number and approach gently to asymptote values. The separated flow deflected angle, the upstream separation distance, the position of the maximum heating point on the plate and the height of the minimum heating point on the cylinder are roughly independent of Mach number and Reynolds number.

The extent of the interaction region and the peak of the heat flux on both the plate and the cylinder are reduced while the cylinder sweeps backward from 0 ° to 30 °.

REFERENCES

1 Войженко Д. М., и другие. Обтекание Цилиндрилеского препятетвия на пластина сверхзвуковый потоком гаэа. и эв., *Акад. Наук. СССР Механика Жидкости и Газа*, 1(1966)

2 Westkaemper JC Turbulent boundary layer separation ahead cylinder. AIAA J, 1968, 6(7)

3 Sedney R & Kitchens, C W Jr Separation ahead protuberance in supersonic turbulent boundary layer. AIAA J, 1977, 15(4)

4 Kaufman L G et al. Shock impingement caused by boundary layer separation ahead of blunt fins. AIAA J, 1973, 11(10)

5 Halpin R N. Step induced boundary layer separation phenomena. AIAA J, 1965, 3(3)

6 Yu H R & Li Z F. The application of thermo-electric analogue network to measurements of surface heat flux. Mechanics & Practice, 1980, 2(1). (in Chinese)

7 Truitt R W. Hypersonic turbulent boundary layer interaction heat transfer in vicinity of protuberances. AIAA J, 1965, 3(9)

8 Burbank P B et al. Heat transfer and pressure measurements on a flat plate surface and heat transfer measurement on attached protuberance in a supersonic turbulent boundary layer at Mach number of 2.65, 3.57 and 4.44. NASA TN D-1372, 1962

9 Price E A & Stallings R L Jr. Investigation of turbulent separation flows in the vicinity of fin type protuberance at supersonic Mach numbers. NASA TN D-3804, 1967

10 Billing E S. Shock wave shapes around spherical and cylindrical nosed bodies. J Spacecraft Rockets, 1967, 4: 822—823

11 Dolling D S, Cosad C D and Bogdonoff S M. An examination of blunt-fin induced shock wave turbulent boundary layer interaction. AIAA paper 79-068, Jan 1979

12 Hung F T & Clauss J M. Three-dimensional protuberance interference heating in high speed slow. AIAA paper 80-0289, Jan 1980

13 Miller W H. Pressure distribution on single & tandem cylinders mounted on a flat plate in Mach number 5.0 flow. AD-634282, June 1966

14 Lucas E J. Investigation of blunt fin-induced flow separation region on a flat plate at Mach numbers 2.5 to 4.0. AEDC-TR-70-265, Jan 1971

15 Winkelman A E. Experimental investigations of a fin protuberance partially immersed in a turbulent boundary layer at Mach 5. NOLTR-72-33, Jan 1972